Response of Finite Periodic Beam to Turbulent Boundary-Layer Pressure Excitation

R. VAICAITIS*
Columbia University, New York
AND
Y. K. LIN†
University of Illinois, Urbana, Ill.

The response of an N-span Bernoulli-Euler beam on evenly spaced elastic supports and exposed to a convected boundary-layer turbulence is investigated analytically. Transfer matrix technique together with the flexural wave propagation concept is employed for the analysis. The random pressure is decomposed into a field of spatial harmonic plane waves and then the total response is obtained by the superposition of all the infinitesimal responses corresponding to each harmonic wave component. Numerical examples are presented for a five-span beam clamped at both ends. The boundary-layer pressure field is chosen to be a truncated Gaussian white noise moving at a specified convection speed.

I. Introduction

IT is well established by now that the random pressure fluctuations resulting from eddies moving in a boundary-layer turbulent flow can severely excite the exterior of a vehicle traveling at high speed through certain media (air, water). The vibrations so induced will inflict fatigue damage on the structure which must be taken into consideration in the design to ensure that the probability is high for the vehicle to survive its intended service life. To assess the fatigue life, it is necessary to know the statistical properties of the structural response.[1]

The usual construction of a flight vehicle fuselage or a ship hull consists of thin skin reinforced by stiffeners, known as the skin-stringer panel construction. The analysis of actual skin-stringer panels is too complicated; therefore, an idealized model needs to be selected for mathematical treatment. Early papers in the literature on structural response to boundary-layer turbulence were concerned primarily with the noise transmission to the inside of a vehicle. Their model was either a single isolated panel or an infinitely large plate.[2–5] However, these simple models are not suitable for fatigue analysis since the stress spectra computed by use of such models do not exhibit multiple peaks clustered in groups, typical of experimentally determined stress spectra for skin-stringer panels in a broad-band environment. It has been shown that the grouping of stress peaks is due to the interaction between neighboring panels and that a multispan model is required for a realistic analysis.[6] A reasonable idealization is to assume that all panels are identically constructed. Thus, the structural model belongs to a general class of "periodic structures," which possess some interesting common properties.[7] These properties can be explained more readily in the case of a single row of panels or, simpler still, the case of a beam on evenly spaced supports.[8–12] One complication in the use of a multispan model is the extreme tedium and/or inaccuracy in the determination of normal modes [10,11]; therefore, the traditional normal mode approach to compute the total response is not practical for such structures. More recently the response of multispan structures to harmonic and boundary-layer pressure field was considered by Mead and his associate[13,14] using a wave propagation approach originally due to Brillouin.[7] This method seems to work well for periodic structures of an infinite total length or for finite length periodic structures where deflections are zero at all periodically spaced supports.

In this paper we shall consider an N-span Bernoulli-Euler beam on evenly spaced elastic supports and exposed to a convected turbulence field. Both deflections and rotations are allowed at all supports. Since the motion of the beam at each periodic support has two degrees of freedom, two types of flexure waves are present in the beam for which Brillouin's method becomes rather intractable. This difficulty is circumvented by using a transfer matrix formulation.[12,15,16] It will be assumed that the vehicle's speed is sufficiently high that the turbulence field remains nearly unchanged during the time required for an eddy passing the vehicle. In other words, the turbulence field will be idealized as a convected "frozen" random pattern.

II. Problem Formulation

A convected frozen random pressure field may be represented as a superposition of numerous infinitesimal plane waves

$$p(\mathbf{x} - \mathbf{v}t) = \int\int_{-\infty}^{\infty}\int p(\mathbf{k})\exp[i\mathbf{k}\cdot(\mathbf{x} - \mathbf{v}t)]\, d\mathbf{k} \qquad (1)$$

where $\mathbf{k}$ and $\mathbf{v}$ are wave number and velocity vectors, respectively. They are related to the frequency of wave propagation by $\omega = \mathbf{k}\cdot\mathbf{v}$.

Assuming that the random excitation has operated for a sufficiently long time and the effects of initial conditions have died out, the structural response can be written as

$$\mathbf{Z}(\mathbf{x}, t) = \int\int_{-\infty}^{\infty}\int p(\mathbf{k})\mathbf{S}(\mathbf{x},\mathbf{k})e^{-i\mathbf{k}\cdot\mathbf{v}t}d\mathbf{k} \qquad (2)$$

where $\mathbf{Z}$ is a response state vector and from a comparison of Eqs. (1) and (2), it is clear that the vector $\mathbf{S}\exp(-i\mathbf{k}\cdot\mathbf{v}t)$ gives the response at $\mathbf{x}$ due to a unit plane wave $\exp[i\mathbf{k}\cdot(\mathbf{x} - \mathbf{v}t)]$. The column matrix $\mathbf{S}$ will be called the matrix of sensitivity functions.

The matrix of autocorrelations and cross-correlations of the components of the response vector is given by

$$E[\mathbf{Z}(\mathbf{x}_1, t_1)\mathbf{Z}^T(\mathbf{x}_2, t_2)] = \int_{-\infty}^{\infty}\cdots\int E[p(\mathbf{k}_1)p^*(\mathbf{k}_2)]$$
$$\cdot\mathbf{S}(\mathbf{x}_1,\mathbf{k}_1)\mathbf{S}^{*T}(\mathbf{x}_2,\mathbf{k}_2)\cdot\exp[-i(\mathbf{k}_1t_1 - \mathbf{k}_2t_2)\cdot\mathbf{v}]d\mathbf{k}_1d\mathbf{k}_2 \qquad (3)$$

where $E[\ \ ]$ denotes the mathematical expectation, an asterisk indicates the complex conjugate, and a superscript T represents the transpose of a matrix. For a homogeneous turbulence field

Received December 10, 1971; presented as Paper 72-171 at the AIAA 10th Aerospace Sciences Meeting, San Diego, Calif., January 17–19, 1972.
Index categories: Structural Dynamic Analysis; Aeroelaslicity and Hydroelaslicity.
* Assistant Professor of Civil Engineering. Associate Member AIAA.
† Professor of Aeronautical and Astronautical Engineering. Member AIAA.

$$E[p(\mathbf{k}_1)p^*(\mathbf{k}_2)] = \Phi(\mathbf{k}_1)\delta(\mathbf{k}_1 - \mathbf{k}_2) \tag{4}$$

where $\Phi(\mathbf{k})$ is the multidimensional spectral density function in the wave number domain and it is defined as the Fourier transform of the correlation function $R(\mathbf{u})$

$$\Phi(\mathbf{k}) = \frac{1}{(2\pi)^3}\int\int_{-\infty}^{\infty}\int R(\mathbf{u})\exp(-i\mathbf{k}\cdot\mathbf{u})d\mathbf{u} \tag{5}$$

where $\mathbf{u} = \mathbf{x}_1 - \mathbf{x}_2$. Substituting (4) into (3), we have

$$E[\mathbf{Z}(\mathbf{x}_1, t_1)\mathbf{Z}^T(\mathbf{x}_2, t_2)] = \int\int_{-\infty}^{\infty}\int \mathbf{S}(\mathbf{x}_1, \mathbf{k})\cdot\Phi(\mathbf{k})\cdot \mathbf{S}^{*T}(\mathbf{x}_2, \mathbf{k})\exp[-i\mathbf{k}\cdot\mathbf{v}(t_1 - t_2)]d\mathbf{k} \tag{6}$$

The matrix of cross-spectral densities for the components of $\mathbf{Z}$ is obtained by treating the right-hand side of Eq. (6) as a function of $\tau = t_2 - t_1$ and taking the Fourier transform,

$$[\Phi_{zz}(\mathbf{x}_1, \mathbf{x}_2, \omega)] = \int\int_{-\infty}^{\infty}\int \mathbf{S}(\mathbf{x}_1, \mathbf{k})\Phi(\mathbf{k})\cdot\mathbf{S}^{*T}(\mathbf{x}_2, \mathbf{k})\delta(\omega - \mathbf{k}\cdot\mathbf{v})d\mathbf{k} \tag{7}$$

The elements on the ith row and jth column in this matrix is the cross-spectral density of $Z_i(\mathbf{x}_1, t_1)$ and $Z_j(\mathbf{x}_2, t_2)$. The spectral densities are obtained from the diagonal elements by letting $\mathbf{x}_1 = \mathbf{x}_2$. To evaluate the response cross-spectra given in Eq. (7), it is necessary to know the sensitivity function matrix $\mathbf{S}$ and the spectral density of the turbulence field $\Phi(\mathbf{k})$. Equation (7) applies to any linear structure under the excitation of a convected frozen field. In what follows we shall restrict our discussion to a one-dimensional structure and our numerical computation to just spectral densities. Within these restrictions, we only require the formula

$$\Phi_{Z_jZ_j}(x, \omega) = (1/v)\,\Phi(\omega/v)|S_j(x, \omega/v)|^2 \tag{8}$$

where S_j is the jth component of the $\mathbf{S}$ vector.

III. Determination of Sensitivity Function Matrix

Limiting our discussion to a one-dimensional N-span Bernoulli-Euler beam elastically constrained against rotation and translation at uniformly spaced intervals and immersed in a fluid stream as shown in Fig. 1, the sensitivity function matrix can be obtained utilizing the transfer matrix techniques.[12,15,16] The advantage of a transfer matrix formulation includes the ease of imposition of boundary conditions, the consideration of deflection, slope, moment, and shear simultaneously as different components of response vector, and the ability to treat a structure composed of periodic units with very complicated configurations. The last item is illustrated by the attachment of a damping device at the center of each span for the control of response levels.

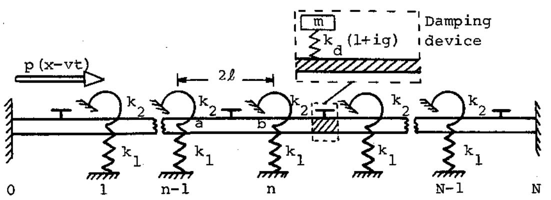

Fig. 1 Problem geometry.

We note some interesting properties of a transfer matrix[12]: 1) the determinant of a transfer matrix is unity; 2) the inversion of a transfer matrix can be accomplished by rearranging the elements and changing some of their signs; 3) the eigenvalues are in reciprocal pairs; 4) if the structural element represented by a transfer matrix is symmetrical, then by a suitable choice of the order and sign convention for the components of the state vector the transfer matrix can be made symmetrical about its cross-diagonal.

We recall that sensitivity functions are related to a plane wave excitation. Then the equation of motion for a uniform beam segment, say, between sections a and b is given by

$$EI\,\partial^4 w/\partial x^4 + \rho A\,\partial^2 w/\partial t^2 = e^{ik(x-vt)} \tag{9}$$

At the steady-state $w(x, t) = W(x, k)e^{-ikvt}$. Then, canceling the common factor $\exp(-ikvt)$ on both sides of Eq. (9), we obtain

$$d^4W/dx^4 - \eta^4 W = e^{ikx}/EI \tag{10}$$

where

$$\eta^4 = (\rho A/EI)(kv)^2$$

Let the distance between a and b be l. Then the solution to Eq. (10) expressed in matrix form is

$$\mathbf{S}_b = \mathbf{F}\mathbf{S}_a + [(\mathbf{F} - e^{ikl}\mathbf{I})/EI(k^4 - \eta^4)]\mathbf{P} \tag{11}$$

where $\mathbf{I}$ is the identity matrix, where $\mathbf{F}$ is a field transfer matrix which would transfer the state vector $\mathbf{S}$ from station a to station b if the beam were unloaded, where $\mathbf{P} = \{-1, -ik, EIk^2, iEIk^3\}$ and where $\mathbf{S}$ is the required sensitivity function matrix with components $S_\delta = W(x, k)$, $S_\theta = dW(x, k)/dx$, $S_M = EId^2W(x, k)/dx^2$, $S_V = EI\,d^3W(x, k)/dx^3$ (corresponding to deflection, slope, moment, and shear, respectively.) By choosing the basic periodic unit for the beam to be symmetric about the center of an interior span, the transfer matrix for an unloaded beam between stations n and $n+1$ of such a basic unit can be written as[12]

$$\mathbf{T} = \mathbf{G}^{1/2}\mathbf{F}\mathbf{D}\mathbf{F}\mathbf{G}^{1/2} \tag{12}$$

where $\mathbf{G}$ is a point transfer matrix associated with an elastic support and $\mathbf{D}$ is associated with damping device attached at the midspan of each periodic beam segment. The use of $\mathbf{G}^{1/2}$ at both ends of the chain product in computing the transfer matrix $\mathbf{T}$ for an unloaded basic periodic unit implies that every interior support is shared by two neighboring units. Matrices $\mathbf{F}$, $\mathbf{G}^{1/2}$, and $\mathbf{D}$ are given in Appendix. From Eqs. (11) and (12), the transfer relation for a loaded basic periodic unit is

$$\mathbf{S}^l_{n+1} = \mathbf{T}\mathbf{S}^r_n + \mathbf{E} \tag{13}$$

where

$$\mathbf{E} = \mathbf{G}^{1/2}(\mathbf{F}\mathbf{D} + \mathbf{I})[(\mathbf{F} - e^{ikl}\mathbf{I})/EI(k^4 - \eta^4)]\mathbf{P} \tag{14}$$

and where the superscript, l or r, signifies that the state vector is evaluated at the left or right of a station. The inhomogeneous difference equation, Eq. (13) can be solved to yield

$$\mathbf{S}_{n+m} = \mathbf{T}^n\mathbf{S}_m + \sum_{r=0}^{n-1}\mathbf{T}^r\mathbf{E} \tag{15}$$

Equation (15) together with boundary conditions at the end stations can be used to determine the sensitivity function matrix at any periodic station† for a periodic beam considered in Fig. 1. For example, let both ends of the beam be clamped. Then from a straight forward matrix operation we obtain, at the periodic station q

$$\mathbf{S}_q = -\begin{bmatrix} u_{13} & u_{14} \\ u_{23} & u_{24} \\ u_{33} & u_{34} \\ u_{43} & u_{44} \end{bmatrix} \frac{\begin{bmatrix} r_{24} & -r_{14} \\ -r_{23} & r_{13} \end{bmatrix}\begin{bmatrix} v_1 \\ v_2 \end{bmatrix}}{r_{13}r_{24} - r_{23}r_{14}} + \begin{bmatrix} h_1 \\ h_2 \\ h_3 \\ h_4 \end{bmatrix} \tag{16}$$

where u_{ij}, r_{ij}, v_i, h_i, are elements from transfer matrices

$$\mathbf{U} = \mathbf{G}^{-1/2}\mathbf{T}^N\mathbf{G}^{-1/2}, \quad \mathbf{R} = \mathbf{T}^r\mathbf{G}^{-1/2}$$

$$\mathbf{V} = \mathbf{G}^{-1/2}\left(\sum_{r=0}^{N-1}\mathbf{T}^r\mathbf{E}\right), \quad \mathbf{H} = \sum_{r=0}^{q=1}\mathbf{T}^q\mathbf{E},$$

respectively. Note that matrix $\mathbf{G}^{-1/2}$ is used whenever is necessary to remove the effect of a "half" elastic support which has been accounted for in the computation of $\mathbf{T}$ for a basic periodic unit.

The use of Eq. (16) requires determination of matrix $\mathbf{T}^n$. If n is large, the roundoff error accumulated from direct multiplication can be excessive. However, by use of Caley-Hamilton theorem $\mathbf{T}^n$ can be expresses as a linear combination of any four indepen-

† That is, a station marking the boundary of two neighboring units.

dent analytic functions of **T**. It is convenient to choose the form[12]

$$\mathbf{T}^n = \sum_{j=1}^{2} \left(a_j \frac{\mathbf{T}^j + \mathbf{T}^{-j}}{2} + b_j \frac{\mathbf{T}^j - \mathbf{T}^{-j}}{2} \right) \tag{17}$$

The coefficients a_j and b_j can be determined by substituting the eigenvalues of **T** into Eq. (17). Let these eigenvalues be $\exp(\pm i\theta_1)$ and $\exp(\pm i\theta_2)$ where $\theta_1 \neq \theta_2$. The simultaneous equations for a_j and b_j are found to be

$$\cos n\theta_m = \sum_{j=1}^{2} a_j \cos j\theta_m \tag{18a}$$

$m = 1,2$

$$\sin n\theta_m = \sum_{j=1}^{2} b_j \sin j\theta_m \tag{18b}$$

If $\theta_1 = \theta_2 = \theta$, Eq. (18) must be replaced by

$$\cos n\theta = \sum_{j=1}^{2} a_j \cos j\theta \tag{19a}$$

$$n \sin n\theta = \sum_{j=1}^{2} j a_j \sin j\theta \tag{19b}$$

$$\sin n\theta = \sum_{j=1}^{2} b_j \sin j\theta \tag{19c}$$

$$n \cos n\theta = \sum_{j=1}^{2} j b_j \cos j\theta \tag{19d}$$

The eigenvalues are generally complex. They are obtained from the characteristic equation for **T**

$$\lambda^4 - 2K_1\lambda^3 + 2K_2\lambda^2 - 2K_1\lambda + 1 = 0 \tag{20}$$

where

$$K_1 = \tfrac{1}{2} \sum_{i=1}^{4} t_{ii}$$

$$K_2 = \tfrac{1}{4} \sum_{i=1}^{4} \sum_{\substack{j=1 \\ i \neq j}}^{4} (t_{ii}t_{jj} - t_{ij}t_{ji}) \tag{21}$$

and t_{ij} are elements of transfer matrix **T**. Note that the coefficients in Eq. (20) are symmetric, typical for periodic structures. Substituting $\lambda = \exp(\pm i\theta_j)$ $(j = 1,2)$ into Eq. (20), it can be shown that

$$\left.\begin{matrix}\cos\theta_1 \\ \cos\theta_2\end{matrix}\right\} = \frac{K_1}{2} \pm \left(\frac{K_1^2}{4} - \frac{K_2 - 1}{2} \right)^{1/2} \tag{22}$$

The summation

$$\sum_{r=0}^{n-1} \mathbf{T}^r$$

can be carried out in a similar manner. Write

$$\sum_{r=0}^{n-1} \mathbf{T}^r = \sum_{j=1}^{2} \left(c_j \frac{\mathbf{T}^j + \mathbf{T}^{-j}}{2} + d_j \frac{\mathbf{T}^j - \mathbf{T}^{-j}}{2} \right) \tag{23}$$

The coefficients c_j and d_j can be determined from

$$\sin(r\theta_m/2)\cos[(r-1)\theta_m/2] = \sin(\theta_m/2) \cdot \sum_{j=1}^{2} c_j \cos j\theta_m \tag{24a}$$

$m = 1,2$

$$\sin(r\theta_m/2)\sin[(r-1)\theta_m/2] = \sin(\theta_m/2) \cdot \sum_{j=1}^{2} d_j \sin j\theta_m \tag{24b}$$

Numerical difficulty may arise when evaluating the denominator $r_{13}r_{24} - r_{14}r_{23}$ in Eq. (16). Since in most practical cases the interior elastic supports are rather stiff, the elements of matrix **R** can become quite large. At or near each response peak $r_{13}r_{24} - r_{14}r_{23}$ is a small difference of two very large numbers. Thus, a more accurate procedure for the computation of this denominator is often required. Such a procedure is available in the method of delta matrices.[12,15]

The sensitivity function matrix, Eq. (16), is evaluated at a demarcation point of two neighboring periodic units. Such a demarcation point is "artificial" since we have artificially split the contribution of an elastic support between two units for mathematical convenience. However, it is a simple matter to evaluate this matrix at any other station once its value at the nearest periodic station is known. For example, at the right of support q we have

$$\mathbf{S}_q^r = \mathbf{G}^{-1/2}\mathbf{S}_q \tag{25}$$

and at the left of the damper between supports q and $q+1$, we have from Eq. (11)

$$\mathbf{S} = \mathbf{F}\mathbf{S}_q^r + (EI)^{-1}(k^4 - \eta^4)^{-1}[\mathbf{F} - e^{ikl}\mathbf{I}]\mathbf{P} \tag{26}$$

The special case where the translational degree of freedom is prohibited, considered by Mead and his associate,[13,14] belongs to a general class of "interior singular conditions."[12] It can be shown that under such conditions the analysis of the problem is simplified considerably since the order of transfer matrix is reduced from 4×4 to 2×2. Denoting the transfer matrix for a basic periodic unit by **B**, the sensitivity function matrix for a beam with such an "interior singular condition" is

$$\bar{\mathbf{S}}_{n+m} = \mathbf{B}^n\bar{\mathbf{S}}_m + \sum_{r=0}^{n-1} \mathbf{B}^r \bar{\mathbf{E}} \tag{27}$$

where

$$\bar{\mathbf{S}} = \{S_\beta, S_M\}, \quad \bar{e}_1 = e_2 - e_1 t_{24}/t_{14}, \quad \bar{e}_2 = e_3 - e_1 t_{34}/t_{14} \tag{28}$$

and e_j are the elements of the column matrix **E** given in Eq. (14). The elements of matrix **B** can be computed from the elements of matrix **T** as follows:

$$b_{11} = (t_{14}t_{22} - t_{12}t_{24})/t_{14} \tag{29a}$$

$$b_{12} = (t_{14}t_{23} - t_{13}t_{24})/t_{14} \tag{29b}$$

$$b_{21} = (t_{14}t_{32} - t_{12}t_{34})/t_{14} \tag{29c}$$

$$b_{22} = (t_{14}t_{33} - t_{13}t_{34})/t_{14} \tag{29d}$$

Matrix **B** possesses the usual properties of a transfer matrix and it is cross-symmetric whenever **T** is cross-symmetric.

Matrices $\mathbf{B}^n$ and

$$\sum_{r=0}^{n-1} \mathbf{B}^n$$

can be evaluated in a similar fashion as before by applying the Caley-Hamilton theorem

$$\mathbf{B}^n = \cos n\theta/\cos\theta[(\mathbf{B} + \mathbf{B}^{-1})/2] + \sin n\theta/\sin\theta[(\mathbf{B} - \mathbf{B}^{-1})/2] \tag{30}$$

$$\sum_{r=0}^{n-1} \mathbf{B}^n = \frac{\sin(n\theta/2)\cos[(n-1)\theta/2]}{\sin(\theta/2)\cos\theta}\left(\frac{\mathbf{B} + \mathbf{B}^{-1}}{2}\right) + \frac{\sin(n\theta/2)\sin[(n-1)\theta/2]}{\sin(\theta/2)\sin\theta}\left(\frac{\mathbf{B} - \mathbf{B}^{-1}}{2}\right) \tag{31}$$

IV. Coincidence Phenomenon

For an undamped case, free flexural waves may exist in a periodically supported beam. Every such a wave is propagated at a characteristic speed and a characteristic wave number.[14] When a forcing plane wave and the natural free flexure wave match in both speed and wave number, the condition called "coincidence" occurs. The result is a theoretically unbounded response in the structure. For a finitely long periodic beam under convected boundary-layer turbulence excitation, the "coincidence" phenomenon is evidenced by multiple peaks in the response spectrum clustered in separate zones. These zones roughly coincide with the so-called free wave propagation zones for the corresponding infinite long beam.[14] The number of peaks in each zone is equal to the number of spans of the beam. This is in contrast to the result from a single span model where individual spectral peaks are well separated. When damping is present these peaks are supressed but they remain clustered in groups. The response level usually can be greatly reduced by tuning the midspan dampers to a frequency near the center of an appropriate free wave propagation zone. Thus, such dampers may be tailored to suit a given spectral shape of the boundary-layer turbulence environment.

V. Numerical Examples

Numerical results were obtained for a five-span beam clamped at both ends using a double precision procedure on an IBM 360/91 computer. These results are presented in Figs. 2–4 in terms of spectral densities and rms values of the bending moment at the center of the middle span. The following is a list of physical data used in the computation: $2l = 8.2$ in. (distance between supports); $b = 1$ in. (beam width); $t = 0.04$ in. (beam thickness); $E = 10.5 \times 10^6$ lb/in.^{2} (Young's modulus); $k_1 = 1100.0$ lb/in. (deflectional spring constant); $k_2 = 180.0$ in. $-$ lb/rad (rotational spring constant); $k_d = 1$ lb/in. (spring constant of damper unit); m = mass of damper unit; $\rho = 0.101/386$ lb $-$ sec^2/in.^{4} (beam mass density); $\omega_n = (k_d/m)^{1/2} = 750.0$ rad/sec (natural frequency of damper unit).

Structural damping of the beam material and the elastic supports is accounted for my multiplying complex factors $(1 + ig_{sd})$, $(1 + ig_{des})$, and $(1 + ig_{res})$ to E, k_1, and k_2, respectively. The damper unit attached at severy midspan is tuned at frequency $\omega_n = 750$ rad/sec and each has a loss factor of $g = 0.2$.

The boundary-layer turbulence is assumed to be characterized by a spectral density

$$\Phi(k) = \begin{cases} (2k_c)^{-1}\sigma^2, & -k_c \le k \le k_c \\ 0 & \text{otherwise} \end{cases} \tag{32}$$

where σ^2 is the mean-square pressure and k_c is a cutoff wave number. It is well established that σ varies as the square of the freestream velocity U_∞; that is, $\sigma = \alpha U_\infty^2$. For subsonic flow at an altitude of 25,000 ft a realistic estimate for the constant α is about 2.22×10^{-8} when U_∞ is expressed in fps and σ in psi. The cutoff wave number k_c is chosen so that the energy available in the turbulence is used to excite only those modes within the first free wave propagation zone. Therefore, if this first zone is located in the frequency interval $[\omega_l, \omega_u]$, then k_c is chosen to be slightly greater than ω_u/v. The convection speed is assumed to be 0.8 of the freestream velocity U_∞.

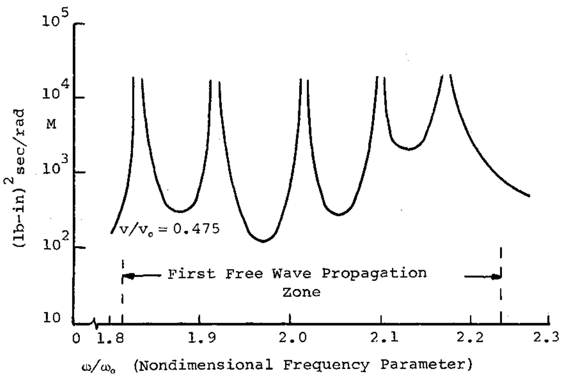

Fig. 2 Spectral density of bending moment (undamped case).

Figure 2 shows the power spectral density of the bending moment M at the center of the middle span when the system is undamped. The abscissa is the excitation frequency normalized to the fundamental natural frequency ω_o (340 rad/sec) of a single span beam simply supported at both ends. The range of excitation frequency shown in the figure covers the whole of the first free wave propagation zone. It is interesting to note that the theoretical response becomes unbounded at the frequencies where free flexural waves in the beam exist; that is, when "coincidence" occurs. In Fig. 3 similar results are shown for a damped system for several convection velocities. The convection velocity v is normalized to the speed of sound in the atmosphere v_0 (1017 fps). In the computation we used $g_{sd} = 0.02$ and $g_{res} = g_{des} = 0.05$. This figure demonstrates that the damping device considered herein can be used effectively to reduce response levels over a wide frequency range. Corresponding to the same physical data as those used to obtain Fig. 3, the rms bending moments (obtained by integrating the response spectral densities over the range of ω for the first free wave propagation zone and then taking the square root) are shown in Fig. 4 for different convection velocities.

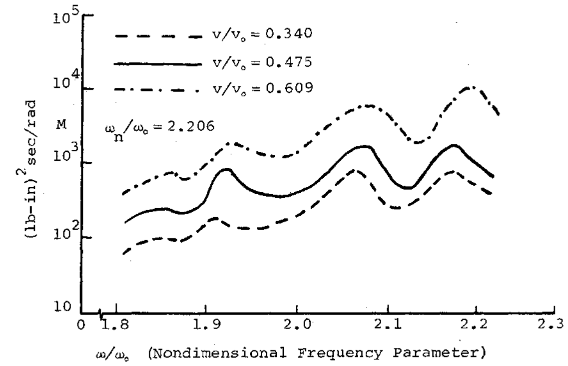

Fig. 3 Spectral density of bending moment (damped case).

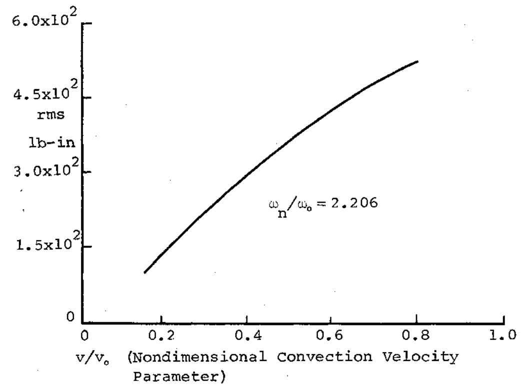

Fig. 4 The rms response of bending moment in the beam.

VI. Conclusions

Although the calculations reported above pertain to a simple Bernoulli-Euler beam, primary conclusions drawn from the present study are believed to apply to all periodic structures under convected noise excitations. The transfer matrix approach used in this study is seen to be a suitable and convenient way in analyzing the response of periodic structures to random pressure fields.

Appendix: Basic Transfer Matrices F, $G^{1/2}$, D

$$\mathbf{F} = \begin{bmatrix} C_0 & lS_1 & l^2C_2/EI & l^3S_3/EI \\ \gamma^4 S_3/l & C_0 & & lS_1/EI \\ \gamma^4 EIC_2/l^2 & \gamma^4 EIS_3/l & & \\ \gamma^4 EIS_1/l^3 & & \text{(cross-symmetric)} & \end{bmatrix} \tag{A1}$$

$$\mathbf{G}^{1/2} = \begin{bmatrix} 1 & 0 & 0 & 0 \\ 0 & 1 & 0 & 0 \\ 0 & k_2^{1/2} & 1 & 0 \\ -k_1^{1/2} & 0 & 0 & 1 \end{bmatrix} \qquad \mathbf{D} = \begin{bmatrix} 0 & 0 & 0 & 0 \\ 0 & 1 & 0 & 0 \\ 0 & 0 & 1 & 0 \\ d & 0 & 0 & 1 \end{bmatrix} \tag{A2}$$

where EI = bending rigidity; $\gamma = l(\mu/EI)^{1/4}\omega^{1/2}$; μ = mass of beam per unit length; $C_o = (\cos h\gamma + \cos\gamma)/2$; $S_1 = (\sin h\gamma + \sin\gamma)/2\gamma$; $C_2 = (\cos h\gamma - \cos\gamma)/2\gamma^2$; $S_3 = (\sin h\gamma - \sin\gamma)/2\gamma^3$; and $d = m\omega^2/[1 - \omega^2 m/k_d(1 + ig)]$.

References

[1] Lin, Y. K., *Probabilistic Theory of Structural Dynamics*, McGraw-Hill, New York, 1967.

[2] Corcos, G. M. and Liepman, H. W., "On the Contribution of Turbulent Boundary Layer to the Noise Inside a Fuselage," TM 1420, 1956, NACA.

[3] Ribner, H. R., "Boundary Layer Induced Noise in the Interior of Aircraft," U.T.I.A. Rept. 37, 1956, Univ. of Toronto, Toronto, Canada.

[4] Kraichnan, R. H., "Noise Transmission from Boundary Layer Pressure Fluctuations," *Journal of the Acoustical Society of America*, Vol. 29, 1957, pp. 65–71.

[5] Dyer, I., "Response of Plates to Decaying and Convecting Random Pressure Field," *Journal of the Accoustical Society of America*, Vol. 31, 1959, pp. 922–928.

[6] Lin, Y. K., "Stresses in Continuous Skin-Stiffened Panels Under Random Loading," *Journal of the Aerospace Sciences*, Vol. 29, 1962, pp. 67–75.

[7] Brillouin, L., *Wave Propagation in Periodic Structures*, Dover, New York, 1953.

[8] Miles, J. W., "Vibrations of Beams on Many Supports," *Journal of Engineering Mechanics Division*, ASCE, Vol. 82, (EMI), Jan. 1956, pp. 1–9.

[9] Lin, Y. K., "Free Vibration of Continuous Skin-Stringer Panels," *Journal of Applied Mechanics*, Vol. 27, Dec. 1960, pp. 669–676.

[10] Lin, Y. K., "Free Vibration of Continuous Beams on Elastic Supports," *International Journal of Mechanical Sciences*, Vol. 4, Oct. 1962, pp. 409–423.

[11] Lin, Y. K., Brown, I. D., and Deutschle, P. C., "Free Vibrations of a Finite Row of Continuous Skin-Stringer Panels," *Journal of Sound and Vibration*, Vol. 1, Jan. 1964, pp. 14–27.

[12] Lin, Y. K. and McDaniel, T. J., "Dynamics of Beam Type Periodic Structures," *Transactions of the ASME: Journal of Engineering for Industry*, Vol. 91, Nov. 1969, pp. 113–1141.

[13] Mead, D. J. and Pujara, K. K., "Space-harmonic Analysis of Periodically Supported Beams; Response to Convected Random Loading," 1970, Inst. of Sound and Vibration Research, Univ. of Southampton, England.

[14] Mead, D. J., "Vibration Response and Wave Propagation in Periodic Structures," Paper 70-WA/DE-3, Jan. 1971, ASME.

[15] Pestel, E. C. and Leckie, F. A., *Matrix Methods in Elastomechanics*, McGraw-Hill, New York, 1963.

[16] Lin, Y. K. and Donaldson, B. K., "A Brief Survey of Transfer Matrix Techniques with Special Reference to the Analysis of Aircraft Panels," *Journal of Sound and Vibration*, Vol. 10, Jan. 1969, pp. 103–143.

Supersonic Flow over Convex and Concave Shapes with Radiation and Ablation Effects

IHOR O. BOHACHEVSKY* AND RONALD N. KOSTOFF †
Bellcomm Inc., Washington, D.C.

A first-order accurate numerical method of unsteady adjustment is employed to calculate inviscid flowfields about convex and concave shapes. Two geometries are used: 1) conical forebodies with spherical afterbodies whose cone half-angles range from 50° to 135° and 2) thin-walled cylinders with cylindrical cavities of different depth facing the oncoming stream. Computations with radiative heat-transfer effects are carried out for flows over 50.56° and 79.83° half-angle cones. A gray gas model is assumed; no restriction is placed on the optical thickness nor is a slab approximation made. Results show a significant departure from the slab approximation near surface discontinuities and large radiative energy losses near cold surfaces. Flows over concave shapes, i.e., the 120° and 135° cones and the two cylinders, relax to their steady-states in a damped oscillatory manner. Higher-order accurate computations are necessary to resolve the nature of these oscillations.

I. Introduction

KNOWLEDGE of the flowfield about a spacecraft entering an atmosphere is important in vehicle design and mission planning. For example, the flowfield determines the dependence of aerodynamic loads and heat-transfer rates (both convective and radiative) on entry trajectory; specification of the charged particle concentration within the flowfield delineates that portion of the entry path where communication blackout occurs. Also, familiarity with the flow pattern assists experimenters in the selection of the most favorable locations on the vehicle surface for placement of their instruments.

Extensive and successful studies of flowfields associated with atmospheric entry vehicles have been performed in the past; the literature pertaining to these investigations is too vast to be discussed here. It is known that, depending on the forebody geometry and the freestream conditions, either of two cases occurs: the shock wave is attached with a supersonic flow behind it, or the shock wave is detached with a mixed subsonic-supersonic flow behind it.

These two cases have always been investigated separately; to the best of our knowledge no method for determining the flowfield exists that does not require prior knowledge of the nature of bow shock configuration. However, as planning and technology become more refined, it becomes desirable to perform flowfield computations for a portion of the trajectory along which the shock configuration changes from attached to detached. Such change of configuration may be caused by the change of freestream conditions or by large ablation rates and excessive blunting of the tip due to erosion.

Recent planning of future space missions envisages extensive use of mass injection from the forebody of the vehicle into the flowfield. This may be either for cooling[1] or, through the application of retrorockets, for assisting in the aerodynamic braking during atmospheric entry.[2] Effective exploitation of these devices

Presented as Paper 71-55 at the AIAA 9th Aerospace Sciences Meeting, New York, January 25–27, 1971; submitted November 3, 1971; revision received February 25, 1972. This work was supported by NASA OMSF under Contract NASW-417.

Index categories: Hypersonic Flows; Radiating Flows; Nonsteady Aerodynamics.

* Member, Technical Staff. Member AIAA.

† Member, Technical Staff.